

Zero-point energy of solids from vacuum fluctuation and quantum geometric force

Yugo Onishi^{1,*} and Liang Fu¹

¹*Department of Physics, Massachusetts Institute of Technology, Cambridge, MA 02139, USA*

(Dated: February 10, 2026)

We show that quantum fluctuations of electromagnetic fields induce an additional zero-point energy in solids, which scales with the volume. For insulators, the zero-point energy density is proportional to quantum fluctuation of electric polarization in the many-body ground state, a fundamental quantum geometric property of solids known as the quantum weight. Although the zero-point energy does not affect the dynamics of the electromagnetic fields, when the fields are produced by a superconducting LC circuit, the zero-point energy contributes to a repulsive force between the circuit and the material. In addition, since zero-point energy depends on the circuit's capacitor, it yields a measurable static force acting on the capacitor plates, which we call quantum geometric force. The proposed effects provide direct experimental access to the many-body quantum geometry and reveal a new macroscopic quantum effect in solids induced by vacuum fluctuation.

Introduction. — A profound consequence of quantum field theory is that the vacuum is not empty. It is filled with fluctuating electromagnetic fields, leading to observable consequences. When coupled to these fluctuating fields, the atomic spectra of an atom experience a shift—called Lamb shift [1–3], and an attractive force between the atoms emerges—known as van der Waals force. These fluctuation-induced spectra shift and force are ubiquitous consequences of quantum electrodynamics (QED).

In this century, developments in microwave cavities offer exciting opportunities to study the interaction between discrete electromagnetic modes and artificial atoms with an unprecedented tunability [4, 5]. The analogy of Lamb shift was observed in a superconducting qubit—an effectively two-level system—coupled to virtual microwave photons in a superconducting resonator [6, 7].

In this work, we study the effect of fluctuating electromagnetic fields on solids containing $\sim 10^{23}$ electrons, and show that the coupling to virtual low-energy photons results in an *increase* of the ground state energy of insulating states. This leads to new phenomena that can be experimentally tested: (1) a *repulsive* force between a dielectric and a microwave resonator that are *inductively* coupled, and (2) a force acting on the capacitor in the microwave circuit.

These predicted phenomena should be contrasted with the Lamb shift [1–3] and Casimir effect [8, 9], which also originate from the vacuum fluctuations. The Lamb shift of the ground state is negative and the Casimir force is typically attractive, whereas we find a positive energy shift and a repulsive force between the solid and the resonator.

Interestingly, the energy shift of an insulator due to its coupling with virtual microwave photons is directly determined by the quantum geometry of the many-body ground state. Since the energy scale of microwave photons is several orders of magnitude smaller than the electronic energy scale in solids, the electronic system is “fast”

compared to the “slow” microwave fields. As a result, the electronic system remains in its instantaneous ground state, but acquires an additional zero-point energy that is extensive in its volume and proportional to the many-body quantum metric. Therefore, we shall call the predicted forces *quantum geometric forces*. Our findings show that superconducting circuits is a powerful new tool for uncovering a fundamental ground state property of quantum materials—the many-body quantum metric—through the quantum geometric force.

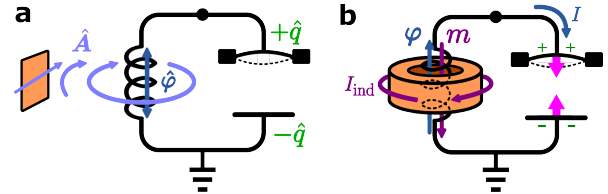


FIG. 1. (a) Interaction between a superconducting LC circuit and a quantum material. The magnetic flux $\hat{\phi}$ behaves as a magnetic dipole moment and creates the vector potential $\hat{\mathbf{A}}$ on the electronic system. (b) The diamagnetic process due to the quantum fluctuation in the superconducting circuit. The flux φ in the inductor induces the current I_{ind} in the electronic system, which results in a magnetic moment m that is antiparallel to the flux φ , and thus increases the energy. The current I accumulates the charge on the capacitor, resulting in an attractive force between the capacitor plates.

Theory. — We consider a general electronic system with a finite energy gap Δ between the ground state $|\Psi_0\rangle$ and the first excited state. Our purpose is to study the effect of the quantum fluctuation of electromagnetic fields on this system in the ground state. In particular, we consider the coupling between the electronic system and electromagnetic fields in a superconducting LC circuit, as illustrated in Fig. 1(a). The total system consisting of the electronic system and the circuit is described by the Hamiltonian given by

$$H_{\text{tot}} = H[\hat{\mathbf{A}}(\mathbf{r}), \hat{\phi}(\mathbf{r})] + H_p, \quad (1)$$

where $H[\hat{\mathbf{A}}(\mathbf{r}), \hat{\phi}(\mathbf{r})]$ is the Hamiltonian of the electronic system in the presence of the vector potential $\hat{\mathbf{A}}(\mathbf{r})$ and the scalar potential $\hat{\phi}(\mathbf{r})$. H_p is the dissipationless Hamiltonian for a superconducting LC circuit that generates the fluctuating electromagnetic field $\hat{\mathbf{A}}(\mathbf{r})$ and $\hat{\phi}(\mathbf{r})$ [10]:

$$H_p = \frac{\hat{\phi}^2}{2L_p} + \frac{\hat{q}^2}{2C_p}, \quad (2)$$

where \hat{q} represents the charge accumulated on the capacitor with the capacitance C_p and $\hat{\phi}$ is the magnetic flux in the inductor with the inductance L_p , which is related to the current \hat{I} as $\hat{\phi} = L_p \hat{I} + \text{const}$. The charge and the magnetic flux satisfy the canonical commutation relation $[\hat{\phi}, \hat{q}] = i\hbar$. By viewing $\hat{\phi}$ as the “position” and \hat{q} as the “momentum”, the Hamiltonian H_p describes a quantum harmonic oscillator with the resonant frequency $\omega_p = 1/\sqrt{L_p C_p}$. Therefore, even in the ground state of the circuit, the charge and the magnetic flux have quantum fluctuations given by $\langle \hat{q}^2 \rangle = \hbar/(2Z_p)$ and $\langle \hat{\phi}^2 \rangle = \hbar Z_p/2$, where $Z_p = \sqrt{L_p/C_p}$ is the characteristic impedance of the circuit.

The fluctuating current and charge in the circuit create vector and scalar potentials that act on the electronic system. From the point of view of electromagnetism, the capacitor acts as an electric dipole moment $P \propto \hat{q}/C_p$ and the inductor acts as a magnetic dipole moment $M \propto \hat{\phi}$. Therefore, we can generally write the potentials created by the LC circuit as

$$\hat{\phi}(\mathbf{r}) = g_C(\mathbf{r}) \frac{\hat{q}}{C_p}, \quad (3a)$$

$$\hat{\mathbf{A}}(\mathbf{r}) = \mathbf{g}(\mathbf{r}) \hat{\phi}, \quad (3b)$$

where the strengths of electric coupling $g_C(\mathbf{r})$ and magnetic coupling $\mathbf{g}(\mathbf{r})$ are spatially varying and depend on the distance to the capacitor and inductor, respectively. Note that we chose the gauge so that $\langle \hat{\mathbf{A}} \rangle = 0$ when $\langle \hat{\phi} \rangle = 0$.

When the size of the electronic system is small compared to the size of the LC circuit, the electromagnetic fields $\hat{\phi}(\mathbf{r})$ and $\hat{\mathbf{A}}(\mathbf{r})$ are approximately uniform within the system. In this case, g_C and \mathbf{g} correspond to the mutual capacitance $C_m \sim g_C/C_p$ and the mutual inductance $M \sim lL_p \mathbf{g}$, where l is the linear size of the electronic system. While a constant potential $\hat{\phi}$ has no physical effect on a system of zero net charge, a fluctuating uniform vector potential cannot be gauged away and has physical consequences, as we show below.

To analyze the Hamiltonian (1), we employ the adiabatic approximation. Since energy gap of an electronic system is generally much larger than the energy scale of the probe $\omega_p \lesssim 10 \text{ GHz} \sim 10 \text{ meV}$, the electronic system is “fast” compared to the “slow” degree of freedom of the LC circuit, and therefore remains in the ground state corresponding to the instantaneous value of φ . Under the

adiabatic condition $\Delta \gg \hbar\omega_p$, we can obtain the effective Hamiltonian by performing a unitary transformation $U(\mathbf{A})$ that diagonalizes $H(\mathbf{A})$:

$$U^\dagger(\mathbf{g}\hat{\phi}) H_{\text{tot}} U(\mathbf{g}\hat{\phi}) = E(\mathbf{g}\hat{\phi}) + \frac{\hat{\phi}^2}{2L_p} + \frac{(q - \hbar\mathbf{g} \cdot \mathbf{a})^2}{2C_p} \quad (4)$$

where $E(\mathbf{A})$ is the ground state energy of $H(\mathbf{A})$, and $\mathbf{a} = iU^\dagger \nabla_{\mathbf{A}} U$ is the (non-Abelian) Berry connection associated with the ground state of $H(\mathbf{A})$. Then, by projecting onto the ground state of the electronic system, we obtain the effective Hamiltonian as

$$H_{\text{eff}} = E_0(\mathbf{g}\hat{\phi}) + \frac{\hat{\phi}^2}{2L_p} + \frac{(\hat{q} - q_0)^2}{2C_p} + E_{\text{QG}} \quad (5a)$$

$$E_{\text{QG}} = \frac{e^2}{2C_p} \mathbf{g} \mathbf{G} \mathbf{g} \quad (5b)$$

where $E_0(\mathbf{A})$ is the ground state energy of $H(\mathbf{A})$, $q_0 = \hbar\mathbf{g} \cdot \mathbf{a}_{00}$ with $\mathbf{a}_{00} = \langle \Psi_0(\mathbf{A}) | i \nabla_{\mathbf{A}} | \Psi_0(\mathbf{A}) \rangle$ is the Berry connection associated with the ground state, and the tensor \mathbf{G}_{ij} is the quantum metric [11–14] of the many-body ground state as a function of the vector potential:

$$G_{ij} = \left(\frac{\hbar}{e} \right)^2 \text{Re} \left[\left\langle \frac{\partial \Psi_0}{\partial A_i} \right| (1 - P_0) \left| \frac{\partial \Psi_0}{\partial A_j} \right\rangle \right]. \quad (6)$$

Here $P_0 = |\Psi_0\rangle\langle\Psi_0|$ is the projection operator onto the ground state. Note that $G_{ij} \propto \hbar^2$ vanishes in the limit $\hbar \rightarrow 0$.

E_{QG} in Eq. (5a) emerges as the quantum correction to the adiabatic approximation. When \mathbf{A} is treated as classical and slowly-varying, the electronic ground state adiabatically follows the changing vector potential \mathbf{A} . Once the vector potential $\hat{\mathbf{A}} = \mathbf{g}\hat{\phi}$ fluctuates quantum mechanically and couples to electrons in solids, the true ground state of the whole system is an entangled state of electrons and photons. Correspondingly, the ground state energy acquires a positive shift E_{QG} that is proportional to the quantum metric of the electronic system.

Importantly, E_{QG} is finite even when the expectation value of electromagnetic fields vanishes. Only in the limit $C_p \rightarrow \infty$ where the flux φ and therefore \mathbf{A} becomes classical, the zero-point energy $E_{\text{QG}} \propto 1/C_p$ vanishes. Therefore, the zero-point energy E_{QG} of the electronic system relies on quantum fluctuation in the electromagnetic field to which it couples. This should be contrasted to the standard electromagnetic properties of materials such as optical conductivity, where the applied electromagnetic fields are treated as classical.

For systems with open boundary, the ground state under uniform \mathbf{A} is related to the one under $\mathbf{A} = 0$ through the gauge transformation $|\Psi_0(\mathbf{A})\rangle = e^{ie\mathbf{A} \cdot \mathbf{R}/\hbar} |\Psi_0(0)\rangle$, where $\mathbf{R} = \sum_n \mathbf{r}_n$ is the dipole moment operator of the electrons in the system. Using this relation, we can show that the many-body quantum metric is independent of \mathbf{A} and given by

$$G_{ij} = \langle (R_i - \langle R_i \rangle)(R_j - \langle R_j \rangle) \rangle. \quad (7)$$

Therefore, E_{QG} can be expressed as

$$E_{\text{QG}} = \frac{\langle (\mathbf{g} \cdot \Delta \mathbf{P})^2 \rangle}{2C_p} \quad (8)$$

with $\Delta \mathbf{P} \equiv \mathbf{P} - \langle \mathbf{P} \rangle$ and the total polarization $\mathbf{P} \equiv e\mathbf{R}$.

Eqs. (5a), (5b), and (8) are the first main results of this work, establishing the effect of quantum vacuum fluctuation in a LC circuit on an electronic system. In the case of a single atom, \mathbf{P} in Eq. (8) is simply the electric dipole moment, and E_{QG} reduces to the dipole self-energy discussed in nonrelativistic QED [15, 16]. As we show below, for a macroscopic system, G and therefore the zero-point energy E_{QG} scale with its volume.

The physical picture for zero-point energy E_{QG} is as follows. Polarization fluctuation of the electronic system (an atom or a solid) induces fluctuating current in the circuit through the inductive coupling, which in turn enhances quantum charge fluctuation on the capacitor and therefore increases the energy stored in the capacitor.

We emphasize that the positive zero-point energy E_{QG} is a consequence of the inductive coupling (a current in the circuit induces a current in the electronic system) and is closely related to diamagnetism. To see this, let us consider a case where the electronic system forms a cylinder, and the inductor threads through the cylinder, as shown in Fig. 1(b). In this case, the current along the circumferential direction can be viewed as a magnetic moment m . Therefore, the inductive coupling is equivalent to the coupling between magnetic moments of the electronic system and the circuit. When the capacitance C_p is finite, the current in the circuit is fluctuating. When the inductor produces a fluctuating flux φ , the electronic system responds *diamagnetically* to oppose the change in the flux (Lenz's law), leading to an increase in the energy of the system.

Since E_{QG} is always positive, it contributes to a *repulsive* force between the electronic system and the superconducting circuit. Since the coupling \mathbf{g} is larger at shorter distance between the electronic system and the inductor, the energy E_{QG} increases as they get closer, resulting in a repulsive force. This force is an analog of the Casimir force but is repulsive. As discussed above, this effect can be viewed as the diamagnetic Casimir force [17–19]. Because this repulsive force is directly related to the quantum metric of the electronic insulator, we call it quantum geometric force.

The positive energy shift E_{QG} and the repulsive force should be contrasted with the Lamb shift of an atom [1–3] and the van der Waals or Casimir force [8, 9, 20], where the quantum fluctuation of electromagnetic fields typically results in *negative* ground state energy correction and an *attractive* force between two atoms or macroscopic bodies. This difference can be traced to their different origins. The Lamb shift and related phenomena originate from the dielectric response; the system develops

electric polarization in response to an fluctuating electric field, thus lowering its energy by $\Delta E \sim -\chi \langle E^2 \rangle$, where χ is the polarizability of the system and $\langle E^2 \rangle$ is the fluctuation of the electric field. Notably, this contribution is suppressed in the low frequency limit $\omega_p \rightarrow 0$, since the electric field fluctuation is suppressed in this limit as $\langle E^2 \rangle = g^2 \hbar \omega_p (n_p + 1/2)/C_p$. In our formalism, these dielectric contributions can be derived as a nonadiabatic correction of order $\mathcal{O}(\hbar \omega_p / \Delta)$ and thus small compared to E_{QG} in the low frequency regime, as discussed in Supplemental Materials (SM).

The zero-point energy E_{QG} has another measurable consequence. Since E_{QG} depends on C_p , it induces an attractive force acting on the capacitor of the circuit, which is another manifestation of quantum geometric force. For a capacitor made of two parallel metal plates of area S separated by distance d , the capacitance is given by $C_p = \epsilon S/d$ where ϵ is the dielectric constant of the medium between the plates. Then, the force acting on the capacitor in a circuit state with n_p photons is given by $F \equiv \partial E_{n_p} / \partial d$ where E_{n_p} is the total energy with n_p photons, yielding

$$F = F_{n_p} + \frac{e^2}{2\epsilon S} \mathbf{g} G \mathbf{g} = F_{n_p} + F_{\text{QG}}. \quad (9)$$

Here, $\langle \dots \rangle$ is the expectation value in the ground state, and the sign of F is chosen such that $F > 0$ represents the attractive force between the capacitor plates. $F_{n_p} = \hbar \omega_p (n_p + 1/2)/(2d)$ is the force without the interaction between the electrons and the circuit, which arises from the C_p dependence of the resonant frequency ω_p .

Eq. (9) is the second main result of this work. The second term F_{QG} in Eq. (9) represents the force arising from the electronic system coupled to fluctuating electromagnetic fields: it is proportional to the many-body quantum metric of the electronic system, and does not depend on the state of photons in the circuit. Even when the system is at finite temperature T , the temperature only affects F_p and does not affect F_{QG} , as long as the temperature T is low compared to the electronic system's energy gap.

It is important that the force acting on the capacitor F arises only from the electromagnetic mode that couples to the charge on the capacitor. We note that in addition to the fundamental mode of the LC circuit, there are infinitely many other modes of fluctuating electromagnetic fields, including vacuum fluctuations (spanning all frequency ranges) or those from possible surrounding circuits. While the interaction of the electronic system with these modes also contributes to the shift of the ground state energy, these fields from other sources do not couple appreciably to the capacitor of the LC circuit, and therefore they do not contribute significantly to the force F . By measuring the force F acting on the capacitor, we can isolate only the contribution from a single electromagnetic mode, which allows us to observe the quantum

geometric force in a controlled way.

Importantly, the energy shift E_{QG} and the resulting forces can occur even in a macroscopic system that involves $\sim 10^{23}$ electrons and are extensive in the system volume Ω , because G_{ij} for macroscopic systems with an energy gap is extensive. To see this, consider an atomic insulator where electrons are tightly bound so that the orbital spread ΔR is much smaller than the lattice constant a ($\Delta R \ll a$) and the hopping across the orbitals is negligible. Then, since this system is essentially a collection of independent atoms, the quantum metric G reduces to the sum of each atom's quantum metric and thus is extensive.

More generally, for band insulators in d -dimensions, the many-body quantum metric G is independent of \mathbf{A} and can be expressed in terms of the quantum metric of Bloch wavefunctions at each \mathbf{k} point [21, 22]:

$$G_{ij} = \Omega \text{Re} \int \frac{d^d k}{(2\pi)^d} \langle \partial_{k_i} u(\mathbf{k}) | (1 - P(\mathbf{k})) | \partial_{k_j} u(\mathbf{k}) \rangle \quad (10)$$

where $P(\mathbf{k}) = |u(\mathbf{k})\rangle\langle u(\mathbf{k})|$, $|u(\mathbf{k})\rangle = |u_1(\mathbf{k}) \dots u_r(\mathbf{k})\rangle$ is the Slater determinant state of all the r occupied Bloch states at \mathbf{k} . The corresponding intensive quantity in this case,

$$K_{ij} = \frac{2\pi}{\Omega} G_{ij}, \quad (11)$$

is a ground state property that characterizes long-wavelength density fluctuation, recently termed as quantum weight [22].

For real solids where electrons interact with long-range Coulomb forces, the effect of dielectric screening needs to be considered in understanding the change of the many-body ground state with the vector potential [23]. On the other hand, for two-dimensional materials with an energy gap, because dielectric screening is absent at long wavelength ($q \rightarrow 0$), the relation (11) between many-body quantum metric G and the quantum weight K continues to hold, where K is defined in terms of the static structure factor in the $q \rightarrow 0$ limit [22]:

$$K_{ij} = \frac{\pi}{\Omega} \left. \frac{\partial \langle n_{\mathbf{q}} n_{-\mathbf{q}} \rangle}{\partial q_i q_j} \right|_{\mathbf{q} \rightarrow 0}, \quad (12)$$

where $n_{\mathbf{q}} = \int d\mathbf{r} e^{-i\mathbf{q} \cdot \mathbf{r}} n(\mathbf{r})$ is the number density operator with wavevector \mathbf{q} .

A nontrivial example is a (fractional) Chern insulator with a quantized Hall conductivity [24, 25]. The quantum weight K in (fractional) Chern insulators has a topological bound set by the Chern number \mathcal{C} : $\text{Tr } K \geq |\mathcal{C}|$ [26]. Also, the quantum weight generally diverges in one- and two-dimensional systems near gap closing transition [27]. Therefore, we expect an enhancement in the zero-point energy E_{QG} near topological phase transitions.

By measuring the quantum geometric force F_{QG} , we can directly probe the quantum geometry of solids. Previously, k -space single-particle quantum metric was measured in solids with two-band effective Hamiltonians [28, 29]. For more general systems, methods relying on sum rules requiring broad-frequency measurements [21, 22, 30], or equivalent time domain protocols [31] were proposed, and sum-rule-based measurements of quantum weight have been reported recently [32, 33]. In contrast, the quantum geometric force provides a direct and static probe of the quantum weight in general gapped systems, including interacting systems.

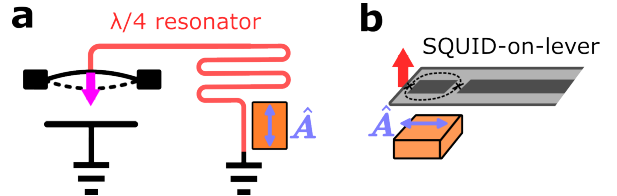


FIG. 2. A possible experimental realization. (a) Measurement of the attractive quantum geometric force. The capacitor in the circuit is made of a mechanical resonator, so that it can move and detect the quantum geometric force. (b) Measurement of the repulsive quantum geometric force. SQUID is fabricated on a cantilever (SQUID-on-lever). SQUID acts as a LC circuit approximately, and the quantum fluctuation in SQUID induces the repulsive quantum geometric force when it is close contact to the material.

Experimental setup. — Possible experimental setups are shown in Fig. 2. To measure the attractive quantum geometric force, we can use a capacitor made of a microelectromechanical resonator [34] as shown in Fig. 2(a). The plates of the capacitor then can move and thus detect the quantum geometric force acting on it. A superconducting circuit coupled to a micromechanical resonator was previously realized in experiments [35, 36]. To realize large inductive coupling, we can place the material near the grounded end of the $\lambda/4$ resonator forming the LC circuit, where the fluctuating current is large. We can also deposit the superconducting wire on the material to maximize the coupling, as done in previous experiments [37].

We estimate the size of \mathbf{g} in this case with a typical mutual inductance M as $\mathbf{g} \sim M/(lL_p) \sim 0.1 \text{ mm}^{-1}$ for $l \sim 1 \text{ mm}$, $M \sim 1 \text{ nH}$ and $L_p \sim 10 \text{ nH}$. For the system volume $\Omega = 1 \text{ mm}^3$, the quantum weight $K \sim 1 \text{ \AA}^{-1}$, and the capacitance $C_p = 100 \text{ fF}$, the zero-point energy is $E_{\text{QG}} \sim 0.1 \text{ eV}$. For the capacitor made of two parallel plates with area $S \simeq 100 \mu\text{m}^2$ separated by a vacuum gap, we estimate $F_{\text{QG}} \sim 10 \text{ pN}$. Both E_{QG} and F_{QG} are significantly large compared to the typical energy scale of a superconducting circuit $\hbar\omega_p \sim 10 \mu\text{eV}$ and the photon-induced force $F_{n_p} \sim 1 \text{ fN}$ for $n_p \sim 1$. The quantum geometric force F_{QG} is within the measurable range of current experimental techniques of microelectromechani-

cal systems, where force sensitivity of $390 \text{ zN Hz}^{-1/2}$ has been achieved [38].

For measurement of the repulsive quantum geometric force, we can use an SQUID instead of the LC circuit as shown in Fig. 2(b). We can consider the Josephson junction in the SQUID as a (nonlinear) inductor with an effective capacitance, thus acting as an LC circuit. We note that the zero-point energy (5b) does not change for nonlinear inductor such as Josephson junction. By measuring the force acting on the SQUID, we can measure the repulsive quantum geometric force. Such a force measurement may be realized by the SQUID-on-Lever technique [39, 40], where a SQUID is fabricated on the cantilever of the atomic force microscopy.

In this case, we can estimate the coupling constant g using the formula for the magnetic moment in magnetostatics: $\mathbf{A} \sim \mu_0 I A / (4\pi R^2)$, where μ_0 is the vacuum permeability, I is the current in the probe, A is the area enclosed by the current path, and R is the distance between the probe and the target system. This yields $g \sim \mu_0 A / (4\pi R^2 L_p) \sim 10 \text{ mm}^{-1}$ for $A \sim 1 \mu\text{m}^2$, $R \sim 100 \text{ nm}$ and $L_p \sim 10 \text{ nH}$. For the capacitance $C_p = 10 \text{ fF}$ and a system with volume $\Omega \sim 1 \mu\text{m}^3$, $K \sim 1 \text{ \AA}^{-1}$, the zero-point energy is $E_{\text{QG}} \sim 1 \text{ \mu eV}$ and the resulting repulsive quantum geometric force is $\nabla E_{\text{QG}} \sim E_{\text{QG}} / R \sim 1 \text{ fN}$.

Lastly, we note that our theory apply also to two coupled superconducting circuits as discussed in SM.

Discussion. — The zero-point energy E_{QG} and the resulting forces are essentially ground state phenomena. They can occur even when the circuit does not excite any real photons. Only through virtual photons, the electrons in solids induce the zero-point energy E_{QG} and results in the repulsive and attractive quantum geometric forces. Our discussion also shows that the many-body quantum metric naturally emerges when both the electronic systems and the electromagnetic fields are quantum mechanical. This is in sharp contrast to the previously discussed effect associated with the Berry curvature [41, 42], or more generally the quantum geometry [21, 26, 27, 30, 31, 43–50], which treated electromagnetic fields classically.

Similar phenomena may occur in other setups beyond the superconducting LC circuit. For example, an optical cavity also has a fluctuating electromagnetic field which can be coupled to quantum materials [4]. Even when the cavity is in the vacuum state, the quantum fluctuation of the electromagnetic field inside the cavity would induce the zero-point energy E_{QG} similar to the superconducting circuit case, although it can involve multiple modes with different frequencies in the cavity.

The effects proposed in this work highlight a new form of interplay between quantum materials and superconducting circuits, and suggest these circuits as a powerful approach to probe and exploit fundamental properties of quantum materials.

We thank Miuko Tanaka, Joel I.-j. Wang, Leonid Glazman and Daniil Antonenko for useful discussions. YO was supported in part by Grant No. NSF PHY-1748958 to the Kavli Institute for Theoretical Physics (KITP), the Heising-Simons Foundation, and the Simons Foundation (216179, LB). LF was supported by the Air Force Office of Scientific Research under award number FA2386-24-1-4043.

* yugo0o24@mit.edu

[1] W. E. Lamb and R. C. Retherford, Fine Structure of the Hydrogen Atom by a Microwave Method, *Physical Review* **72**, 241 (1947).

[2] H. A. Bethe, The Electromagnetic Shift of Energy Levels, *Physical Review* **72**, 339 (1947).

[3] T. A. Welton, Some Observable Effects of the Quantum-Mechanical Fluctuations of the Electromagnetic Field, *Physical Review* **74**, 1157 (1948).

[4] S. Haroche, *Exploring the Quantum: Atoms, Cavities and Photons*, Oxford Graduate Texts (Oxford University Press, Oxford, 2006).

[5] A. Blais, A. L. Grimsom, S. M. Girvin, and A. Wallraff, Circuit quantum electrodynamics, *Reviews of Modern Physics* **93**, 025005 (2021).

[6] A. Fragner, M. Göppl, J. M. Fink, M. Baur, R. Bianchetti, P. J. Leek, A. Blais, and A. Wallraff, Resolving Vacuum Fluctuations in an Electrical Circuit by Measuring the Lamb Shift, *Science* **322**, 1357 (2008).

[7] Z. Ao, S. Ashhab, F. Yoshihara, T. Fuse, K. Kakuyanagi, S. Saito, T. Aoki, and K. Semba, Extremely large Lamb shift in a deep-strongly coupled circuit QED system with a multimode resonator, *Scientific Reports* **13**, 11340 (2023).

[8] H. B. G. Casimir and D. Polder, The Influence of Retardation on the London-van der Waals Forces, *Physical Review* **73**, 360 (1948).

[9] H. B. Casimir, On the attraction between two perfectly conducting plates, in *Proc. Kon. Ned. Akad. Wet.*, Vol. 51 (1948) p. 793.

[10] S. M. Girvin, Circuit QED: Superconducting qubits coupled to microwave photons, in *Quantum Machines: Measurement and Control of Engineered Quantum Systems*, edited by M. Devoret, B. Huard, R. Schoelkopf, and L. F. Cugliandolo (Oxford University Press, Oxford, 2014) 1st ed., pp. 113–256.

[11] F. Wilczek and A. Shapere, *Geometric Phases in Physics*, Advanced Series in Mathematical Physics, Vol. 5 (WORLD SCIENTIFIC, 1989).

[12] M. V. Berry and J. M. Robbins, Classical geometric forces of reaction: An exactly solvable model, *Proceedings of the Royal Society of London. Series A: Mathematical and Physical Sciences* **442**, 641 (1997).

[13] Y. Aharonov and A. Stern, Origin of the geometric forces accompanying Berry's geometric potentials, *Physical Review Letters* **69**, 3593 (1992).

[14] T. Ohnishi and N. Nagaosa, Adiabatic Approximation for Path Integrals and Geometrical Potentials, *Journal of the Physical Society of Japan* **76**, 015003 (2007).

[15] C. Cohen-Tannoudji, J. Dupont-Roc, and G. Grynberg, eds., *Atom-Photon Interactions: Basic Processes and Applications*, A Wiley-Interscience Publication (Wiley, New York, NY, 2008).

[16] V. Rokaj, D. M. Welakuh, M. Ruggenthaler, and A. Rubio, Light-matter interaction in the long-wavelength limit: No ground-state without dipole self-energy, *Journal of Physics B: Atomic, Molecular and Optical Physics* **51**, 034005 (2018).

[17] O. Kenneth, I. Klich, A. Mann, and M. Revzen, Repulsive Casimir Forces, *Physical Review Letters* **89**, 033001 (2002).

[18] B. Geyer, G. L. Klimchitskaya, and V. M. Mostepanenko, Thermal Casimir interaction between two magnetodielectric plates, *Physical Review B* **81**, 104101 (2010).

[19] N. Inui, Diamagnetic effect on the Casimir force, *Physical Review A* **83**, 032513 (2011).

[20] S. Y. Buhmann, *Dispersion Forces I: Macroscopic Quantum Springer Tracts in Modern Physics*, Vol. 247 (Springer Berlin Heidelberg, Berlin, Heidelberg, 2012).

[21] I. Souza, T. Wilkens, and R. M. Martin, Polarization and localization in insulators: Generating function approach, *Physical Review B* **62**, 1666 (2000).

[22] Y. Onishi and L. Fu, Quantum weight: A fundamental property of quantum many-body systems, *Physical Review Research* **7**, 023158 (2025).

[23] Y. Onishi and L. Fu, [2024.01] Quantum weight (2024), arXiv:2401.13847 [cond-mat].

[24] D. J. Thouless, M. Kohmoto, M. P. Nightingale, and M. den Nijs, Quantized Hall Conductance in a Two-Dimensional Periodic Potential, *Physical Review Letters* **49**, 405 (1982).

[25] Q. Niu, D. J. Thouless, and Y.-S. Wu, Quantized Hall conductance as a topological invariant, *Physical Review B* **31**, 3372 (1985).

[26] Y. Onishi and L. Fu, Topological Bound on the Structure Factor, *Physical Review Letters* **133**, 206602 (2024).

[27] Y. Onishi and L. Fu, Fundamental Bound on Topological Gap, *Physical Review X* **14**, 011052 (2024).

[28] M. Kang, S. Kim, Y. Qian, P. M. Neves, L. Ye, J. Jung, D. Puntel, F. Mazzola, S. Fang, C. Jozwiak, A. Bostwick, E. Rotenberg, J. Fuji, I. Vobornik, J.-H. Park, J. G. Checkelsky, B.-J. Yang, and R. Comin, Measurements of the quantum geometric tensor in solids, *Nature Physics* 10.1038/s41567-024-02678-8 (2024).

[29] S. Kim, Y. Chung, Y. Qian, S. Park, C. Jozwiak, E. Rotenberg, A. Bostwick, K. S. Kim, and B.-J. Yang, Direct measurement of the quantum metric tensor in solids, *Science* **388**, 1050 (2025).

[30] B. Ghosh, Y. Onishi, S.-Y. Xu, H. Lin, L. Fu, and A. Bansil, Probing quantum geometry through optical conductivity and magnetic circular dichroism, *Science Advances* **10**, eado1761 (2024).

[31] N. Verma and R. Queiroz, Framework to Measure Quantum Metric from Step Response, *Physical Review Letters* **134**, 106403 (2025).

[32] D. Bañut, B. Bradlyn, and P. Abbamonte, Quantum entanglement and quantum geometry measured with inelastic x-ray scattering, *Physical Review B* **111**, 125161 (2025).

[33] D. Bañut, B. Bradlyn, M. D. Collins, and P. Abbamonte, Fundamental Tests of Quantum Geometric Bounds in Ionic and Covalent Insulators using Inelastic X-Ray Scattering (2026), arXiv:2601.19054 [cond-mat].

[34] B. Xu, P. Zhang, J. Zhu, Z. Liu, A. Eichler, X.-Q. Zheng, J. Lee, A. Dash, S. More, S. Wu, Y. Wang, H. Jia, A. Naik, A. Bachtold, R. Yang, P. X.-L. Feng, and Z. Wang, Nanomechanical Resonators: Toward Atomic Scale, *ACS Nano* **16**, 15545 (2022).

[35] J. D. Teufel, T. Donner, D. Li, J. W. Harlow, M. S. Allman, K. Cicak, A. J. Sirois, J. D. Whittaker, K. W. Lehnert, and R. W. Simmonds, Sideband cooling of micromechanical motion to the quantum ground state, *Nature* **475**, 359 (2011).

[36] A. P. Reed, K. H. Mayer, J. D. Teufel, L. D. Burkhardt, W. Pfaff, M. Reagor, L. Sletten, X. Ma, R. J. Schoelkopf, E. Knill, and K. W. Lehnert, Faithful conversion of propagating quantum information to mechanical motion, *Nature Physics* **13**, 1163 (2017).

[37] M. Tanaka, J. I.-j. Wang, T. H. Dinh, D. Rodan-Legrain, S. Zaman, M. Hays, A. Almanakly, B. Kannan, D. K. Elec, K. Watanabe, T. Taniguchi, T. P. Orlando, S. Gustavsson, J. A. Grover, P. Jarillo-Herrero, and W. D. Oliver, Superfluid stiffness of magic-angle twisted bilayer graphene, *Nature* **638**, 99 (2025).

[38] P. Weber, J. Güttinger, A. Noury, J. Vergara-Cruz, and A. Bachtold, Force sensitivity of multilayer graphene optomechanical devices, *Nature Communications* **7**, 12496 (2016).

[39] M. Wyss, K. Bagani, D. Jetter, E. Marchiori, A. Vervelaki, B. Gross, J. Ridderbos, S. Gliga, C. Schönenberger, and M. Poggio, Magnetic, Thermal, and Topographic Imaging with a Nanometer-Scale SQUID-On-Lever Scanning Probe, *Physical Review Applied* **17**, 034002 (2022).

[40] T. Weber, D. Jetter, J. Ullmann, S. A. Koch, S. F. Pfander, K. Kress, A. Vervelaki, B. Gross, O. Kieler, U. Drechsler, P. R. Baral, A. Magrez, R. Kleiner, A. W. Knoll, M. Poggio, and D. Koelle, Advanced SQUID-on-lever scanning probe for high-sensitivity magnetic microscopy with sub-100-nm spatial resolution, *Physical Review Applied* **24**, 054041 (2025).

[41] G. Sundaram and Q. Niu, Wave-packet dynamics in slowly perturbed crystals: Gradient corrections and Berry-phase effects, *Physical Review B* **59**, 14915 (1999).

[42] D. Xiao, M.-C. Chang, and Q. Niu, Berry phase effects on electronic properties, *Reviews of Modern Physics* **82**, 1959 (2010).

[43] Y. Gao, S. A. Yang, and Q. Niu, Field Induced Positional Shift of Bloch Electrons and Its Dynamical Implications, *Physical Review Letters* **112**, 166601 (2014).

[44] A. Gao, Y.-F. Liu, J.-X. Qiu, B. Ghosh, T. V. Trevisan, Y. Onishi, C. Hu, T. Qian, H.-J. Tien, S.-W. Chen, M. Huang, D. Bérubé, H. Li, C. Tzschaschel, T. Dinh, Z. Sun, S.-C. Ho, S.-W. Lien, B. Singh, K. Watanabe, T. Taniguchi, D. C. Bell, H. Lin, T.-R. Chang, C. R. Du, A. Bansil, L. Fu, N. Ni, P. P. Orth, Q. Ma, and S.-Y. Xu, Quantum metric nonlinear Hall effect in a topological antiferromagnetic heterostructure, *Science* **381**, 181 (2023).

[45] N. Wang, D. Kaplan, Z. Zhang, T. Holder, N. Cao, A. Wang, X. Zhou, F. Zhou, Z. Jiang, C. Zhang, S. Ru, H. Cai, K. Watanabe, T. Taniguchi, B. Yan, and W. Gao, Quantum-metric-induced nonlinear transport in a topological antiferromagnet, *Nature* **621**, 487 (2023).

[46] J. Ahn, G.-Y. Guo, and N. Nagaosa, Low-Frequency Divergence and Quantum Geometry of the Bulk Photo-

voltaic Effect in Topological Semimetals, Physical Review X **10**, 041041 (2020), arXiv:2006.06709.

[47] J. Ahn, G.-Y. Guo, N. Nagaosa, and A. Vishwanath, Riemannian geometry of resonant optical responses, Nature Physics **18**, 290 (2022).

[48] N. Verma and R. Queiroz, Instantaneous response and quantum geometry of insulators, Proceedings of the National Academy of Sciences **122**, e2405837122 (2025).

[49] I. Komissarov, T. Holder, and R. Queiroz, The quantum geometric origin of capacitance in insulators, Nature Communications **15**, 4621 (2024).

[50] T. Neupert, C. Chamon, and C. Mudry, Measuring the quantum geometry of Bloch bands with current noise, Physical Review B **87**, 245103 (2013).

SUPPLEMENTAL MATERIALS

Equivalence with the many-body quantum geometric tensor defined through the twisted boundary condition

The many-body quantum metric of the ground state is defined with the twisted boundary condition [25], which imposes the many-body wavefunction to satisfy the following boundary condition:

$$\begin{aligned} \Psi_{\kappa}(\dots, \mathbf{r}_{j-1}, \mathbf{r}_j + L\hat{x}, \mathbf{r}_{j+1}, \dots) \\ = e^{i\kappa_x L} \Psi_{\kappa}(\dots, \mathbf{r}_{j-1}, \mathbf{r}_j, \mathbf{r}_{j+1}, \dots), \end{aligned} \quad (13)$$

where L is the system size and κ_x specifies the twist angle along x direction, and similarly for y and z directions. Here, \mathbf{r}_j represents the coordinate of the j -th particle. When $\kappa = 0$, the twisted boundary condition reduces to the periodic boundary condition. To define the many-body quantum geometry, we need an analog of cell-periodic Bloch wavefunction for the many-body wavefunction, which we denote by Φ_{κ} and is defined as

$$\Phi_{\kappa}(\mathbf{r}_1, \mathbf{r}_2, \dots, \mathbf{r}_N) = e^{-i\kappa \cdot \sum_j \mathbf{r}_j} \Psi_{\kappa}(\mathbf{r}_1, \mathbf{r}_2, \dots, \mathbf{r}_N). \quad (14)$$

The wavefunction Φ_{κ} satisfies the periodic boundary condition: $\Phi_{\kappa}(\dots, \mathbf{r}_j + L\hat{x}, \dots) = \Phi_{\kappa}(\dots, \mathbf{r}_j, \dots)$ and similar for the other directions. Φ_{κ} is the eigenstate of the κ -dependent Hamiltonian $H(\kappa) = e^{-i\kappa \cdot \sum_j \mathbf{r}_j} H e^{i\kappa \cdot \sum_j \mathbf{r}_j}$.

The many-body quantum geometric tensor is then defined as

$$Q_{ij} = \frac{2\pi}{V} \left\langle \frac{\partial \Phi_0}{\partial \kappa_i} \left| (1 - P_0) \right| \frac{\partial \Phi_0}{\partial \kappa_j} \right\rangle = K_{ij} - \frac{i}{2} C_{ij}. \quad (15)$$

Here, $P_0 = |\Phi_0\rangle\langle\Phi_0|$ is the projection operator onto the ground state and V is the volume of the system. The real part of Q_{ij} defines the many-body quantum metric $K_{ij} = \text{Re } Q_{ij}$, while the imaginary part defines the many-body Berry curvature $F_{ij} = 2 \text{Im } C_{ij}$ and is related to the Chern number \mathcal{C} in two-dimensional systems as $C_{xy} = \mathcal{C}$. The quantum metric in this particular context was recently termed as quantum weight [22], which we shall also use in this paper.

The quantum weight K_{ij} quantifies the change of the ground state under the change of the twisted boundary condition. Physically, it can be interpreted with an external magnetic flux. When the system forms a ring with circumference L implementing the periodic boundary condition and the magnetic flux Φ is threaded through the ring, the magnetic flux produces a uniform vector potential $\mathbf{A} = \Phi/L$ along the ring. This geometry with uniform vector potential \mathbf{A} is equivalent to the twisted boundary condition with κ related by

$$\mathbf{A} = \frac{\hbar}{e} \kappa, \quad (16)$$

with $e(< 0)$ the charge of an electron. Therefore, the quantum geometric tensor defined with the twisted boundary condition is equivalent to that defined through the vector potential as in the main text, up to the factor in Eq. (16).

Effect of capacitive coupling

In this section, we consider the effect of the capacitive coupling, i.e., the coupling through the scalar potential between the electronic system and the superconducting circuit.

For purely capacitive coupling case with $\mathbf{g}_I = 0$, we can simply treat the capacitive coupling as a perturbation to derive a negative energy shift and an attractive force between the electronic system and the circuit. However, this treatment is not clear how it is related to the adiabatic treatment presented in the main text when both the capacitive and inductive couplings are present.

Here, we present a more general treatment that can handle both couplings on equal footing. We show that, even in the presence of the capacitive coupling, the positive energy shift and the repulsive force originating from the quantum geometry dominates in the adiabatic limit $\hbar\omega_p \ll \Delta$ with the gap of the electronic system Δ . Then, we also show that a negative energy shift and an attractive force appears as the nonadiabatic correction, which is suppressed by the factor $\hbar\omega_p/\Delta$ compared to the adiabatic effect. The resulting negative energy shift and the attractive force can be interpreted as the analog of the van der Waals force in our system.

Effective Hamiltonian

We consider the following total Hamiltonian including both the vector and scalar potential couplings:

$$H_{\text{tot}} = H[\mathbf{A}(\mathbf{r})] + \int d^d r \rho(\mathbf{r})\phi(\mathbf{r}) + H_p, \quad (17)$$

where $H[\mathbf{A}(\mathbf{r})]$ is the Hamiltonian of the electronic system in the presence of the vector potential $\mathbf{A}(\mathbf{r})$, $\rho(\mathbf{r})$ is the charge density operator of the electronic system, and $\phi(\mathbf{r})$ is the scalar potential generated by the circuit. H_p is the Hamiltonian of the circuit, which we model as a single-mode LC resonator as in the main text:

$$H_p = \frac{\hat{\varphi}^2}{2L_p} + \frac{\hat{q}^2}{2C_p}, \quad (18)$$

where $\hat{\varphi}, \hat{q}$ are the flux and charge operators of the resonator, satisfying $[\hat{\varphi}, \hat{q}] = i\hbar$. The vector and scalar potentials generated by the circuit are given by

$$\hat{\phi}(\mathbf{r}) = g_C(\mathbf{r}) \frac{\hat{q}}{C_p}, \quad (19a)$$

$$\hat{\mathbf{A}}(\mathbf{r}) = \mathbf{g}_I(\mathbf{r})\hat{\varphi}, \quad (19b)$$

where $g_C(\mathbf{r}), \mathbf{g}_I(\mathbf{r})$ are the spatial profiles of the scalar and vector potentials generated by the circuit per unit flux/charge.

Before proceeding, we note that the couplings through the scalar and vector potential are related to each other by a gauge transformation. To see this, we consider the following unitary transformation:

$$U_1 = \exp\left(-\frac{i\hat{\varphi}}{\hbar} \int d^d r g_C(\mathbf{r})\rho(\mathbf{r})\right). \quad (20)$$

This unitary transformation induces the gauge transformation for the electrons in the target that translates the scalar potential into the vector potential. For example, the annihilation operator of an electron $\hat{\psi}$ transforms under U_1 as $U_1^\dagger \hat{\psi}(\mathbf{r}) U_1 = e^{-ieg_C(\mathbf{r})\hat{\varphi}/\hbar} \hat{\psi}(\mathbf{r})$, where $e(< 0)$ is the charge of an electron. Therefore, U_1 induces the gauge transformation of the vector potential as $\mathbf{A} \rightarrow \mathbf{A} + \hat{\varphi} \nabla g_C(\mathbf{r})$. On the other hand, U_1 shifts the charge operator q of the probe as

$$U_1^\dagger q U_1 = q - Q_0, \quad (21)$$

$$Q_0 \equiv \int d^d r g_C(\mathbf{r})\rho(\mathbf{r}) \quad (22)$$

where Q_0 represents the charge in the probe induced through the interaction with the target.

With the unitary transformation U_1 , the Hamiltonian (17) is transformed into

$$H'_{\text{tot}} \equiv U_1^\dagger H_{\text{tot}} U_1 = H'[\mathbf{A}(\mathbf{r}) = \mathbf{g}(\mathbf{r})\hat{\varphi}] + H_p, \quad (23)$$

$$H'[\mathbf{A}(\mathbf{r})] = H[\mathbf{A}(\mathbf{r})] - \frac{Q_0^2}{2C_p}, \quad (24)$$

$$\mathbf{g}(\mathbf{r}) = \mathbf{g}_I(\mathbf{r}) + \nabla g_C(\mathbf{r}). \quad (25)$$

Here, H' is the Hamiltonian in the presence of the probe. The charge of the probe partially screens that of the target by Q_0 , reducing the effective interaction within the target by $Q_0^2/(2C_p)$. In the form of Eq. (23), all the interaction effects between the target and probe are through the vector potential $\mathbf{A}(\mathbf{r}) = \mathbf{g}(\mathbf{r})\varphi$ and the screening effect represented by $Q_0^2/(2C_p)$.

Quantum geometric force including the effect of charge coupling

Here we consider the quantum geometric force including the effect of charge coupling. As discussed in the previous section, the screening effect modifies the Hamiltonian of the electronic system as

$$H' = H - \frac{Q_0^2}{2C_p} \quad (26)$$

where the last term represents the screening of the interaction due to the probe. Here, we show that the force on the capacitor of the circuit due to the screening is mostly canceled when the scalar potential generated by the charge \hat{q} on the capacitor is given by Eq. (19a) and g_C does not depend on C_p . This is true when the electronic system is placed between the capacitor plates so that the scalar potential on the electronic system is proportional to the electric field generated by the capacitor, $\mathbf{E} \propto \hat{q}/C_p$.

When the capacitor is made of two parallel metal plates with area S and gap size d , the capacitance is given by $C_p = \epsilon S/d$ and the force acting on the capacitor is given by

$$F = \frac{\partial E_{n_p}}{\partial d} = F_{n_p} + \frac{V}{2\epsilon S} \left(-\frac{\langle Q_0^2 \rangle}{V} + \frac{e^2}{2\pi} \mathbf{g} K' \mathbf{g} \right) \quad (27)$$

Here, $\langle \dots \rangle$ is the expectation value in the ground state, and $F_{n_p} = \hbar\omega_p(n_p + 1/2)/(2d)$ is the force without the interaction with the target system, which arises from the dependence of the resonant frequency ω_p on d .

Now we show that $\langle Q_0^2 \rangle$ is related to K' . We first rewrite Q_0 as

$$Q_0 = \int d^d r g_C(\mathbf{r}) \rho(\mathbf{r}) = \frac{1}{V} \sum_{\mathbf{q}} g_C(-\mathbf{q}) \rho(\mathbf{q}) \quad (28)$$

where $\rho(\mathbf{q}) = \int d^d r e^{-i\mathbf{q} \cdot \mathbf{r}} \rho(\mathbf{r})$, $g_C(\mathbf{q}) = \int d^d r e^{-i\mathbf{q} \cdot \mathbf{r}} g_C(\mathbf{r})$ are the Fourier transform of the charge density operator $\rho(\mathbf{r})$ and $g_C(\mathbf{r})$, and V is the volume of the system. Using this, we find that $\langle Q_0^2 \rangle$ is given by

$$\begin{aligned} \langle Q_0^2 \rangle &= \frac{1}{V^2} \sum_{\mathbf{q}, \mathbf{q}'} g_C(-\mathbf{q}) g_C(-\mathbf{q}') \langle \rho(\mathbf{q}) \rho(\mathbf{q}') \rangle \\ &= \langle Q_0 \rangle^2 + \frac{1}{V} \sum_{\mathbf{q}} |g_C(\mathbf{q})|^2 S(\mathbf{q}) \end{aligned} \quad (29)$$

where $S(\mathbf{q}) = (1/V)(\langle \rho(\mathbf{q}) \rho(-\mathbf{q}) \rangle - \langle \rho(\mathbf{q}) \rangle \langle \rho(-\mathbf{q}) \rangle)$ is the static structure factor. Here we assumed that $g_C(\mathbf{r})$ is slowly varying in space so that $g_C(\mathbf{q})$ has significant weight only near $\mathbf{q} = 0$, and the system is translationally invariant so that $\langle \rho(\mathbf{q}) \rho(\mathbf{q}') \rangle$ is finite only when $\mathbf{q} + \mathbf{q}'$ coincides with a reciprocal lattice vector.

Since the static structure factor is related to the quantum weight as $S(\mathbf{q}) = e^2 \mathbf{q} K' \mathbf{q} / (2\pi)$ for small \mathbf{q} [22], we find that

$$\begin{aligned} \langle Q_0^2 \rangle &= \langle Q_0 \rangle^2 + \frac{e^2}{2\pi V} \sum_{\mathbf{q}} |g_C(\mathbf{q})|^2 q_i K'_{ij} q_j \\ &= \langle Q_0 \rangle^2 + \frac{e^2}{2\pi} \int d^d r (\nabla g_C) K' (\nabla g_C) \end{aligned} \quad (30)$$

$$= \langle Q_0 \rangle^2 + \frac{e^2}{2\pi V} (\nabla g_C) K' (\nabla g_C) \quad (31)$$

where in the last line we assumed that $g_C(\mathbf{r})$ varies slowly in space so that we can approximate ∇g_C as constant. Plugging this into the expression for F (27), we obtain

$$F = F_{n_p} - \frac{\langle Q_0 \rangle^2}{2\epsilon S} + \frac{e^2 V}{4\pi \epsilon S} (-(\nabla g_C) K' (\nabla g_C) + \mathbf{g} K' \mathbf{g}) \quad (32)$$

$$= F_{n_p} - \frac{\langle Q_0 \rangle^2}{2\epsilon S} + \frac{e^2 V}{4\pi \epsilon S} (\mathbf{g}_I K' \mathbf{g}_I + 2(\nabla g_C) K' \mathbf{g}_I) \quad (33)$$

Lastly, we note that Q_0 includes all the charges in the target, including the positive background charge. Therefore, if $g_C(\mathbf{r})$ is slowly varying in space compared to the lattice constant of the target, we have $\langle Q_0 \rangle \simeq 0$. Thus, the force acting on the capacitor is given by

$$F = F_{n_p} + \frac{e^2 V}{4\pi \epsilon S} (\mathbf{g}_I K' \mathbf{g}_I + 2(\nabla g_C) K' \mathbf{g}_I) \quad (34)$$

Remark on systems with long-range Coulomb interaction

In the presence of long-range Coulomb interaction, a more careful discussion is needed to properly take into account the screening effect due to the Coulomb interaction.

To discuss this, we first generalize the quantum weight to finite wavevector \mathbf{q} . We consider the quantum system under an external vector potential with wavevector \mathbf{q} , $\mathbf{A}(\mathbf{r}) = 2 \operatorname{Re}[\mathbf{A}_\mathbf{q} e^{i\mathbf{q}\cdot\mathbf{r}}]/V$. We denote the Hamiltonian under the vector potential by $H(\mathbf{A}_\mathbf{q})$, and the ground state by $|\Psi_0(\mathbf{A}_\mathbf{q})\rangle$. Then, we define the generalized many-body quantum metric as

$$K_{ij}(\mathbf{q}) = 2\pi \left(\frac{\hbar}{e}\right)^2 \operatorname{Re} \left\langle \frac{\partial \Psi_0}{\partial A_{\mathbf{q},i}} \right| (1 - P_0) \left| \frac{\partial \Psi_0}{\partial A_{\mathbf{q},j}} \right\rangle. \quad (35)$$

where $P_0 = |\Psi_0\rangle\langle\Psi_0|$ is the projection operator onto the ground state, and the derivatives are evaluated at $\mathbf{A}_\mathbf{q} = 0$.

As discussed previously, the quantum weight behaves differently in the presence of long-range Coulomb interaction. This can be most clearly seen through its relation to optical responses at finite wavevector \mathbf{q} . We define the optical conductivity at finite wavevector \mathbf{q} as

$$\mathbf{j}(\mathbf{q}, \omega) = \sigma(\mathbf{q}, \omega) \mathbf{E}_{\text{ext}}(\mathbf{q}, \omega), \quad (36)$$

where $\mathbf{j}(\mathbf{q}, \omega)$ is the current density at wavevector \mathbf{q} and frequency ω . Importantly, we define σ as the response to *external* electric field $\mathbf{E}_{\text{ext}}(\mathbf{q}, \omega)$, which does *not* include the screening field from the induced charges. Then, the quantum weight at finite wavevector \mathbf{q} is related to the optical conductivity as

$$\int_0^\infty d\omega \frac{\operatorname{Re} \sigma_{ij}^{\text{abs}}(\mathbf{q}, \omega)}{\omega} = \frac{\hbar}{2V} K_{ij}(\mathbf{q}), \quad (37)$$

where $\sigma^{\text{abs}}(\mathbf{q}, \omega) = (\sigma(\mathbf{q}, \omega) + \sigma(\mathbf{q}, \omega)^\dagger)/2$ is the absorptive part of the optical conductivity with finite \mathbf{q} .

We are interested in the limit of $\mathbf{q} \rightarrow 0$. In systems without long-range Coulomb interaction, the optical conductivity $\sigma(\mathbf{q}, \omega)$ is continuous at $\mathbf{q} = 0$, and therefore we have $\lim_{\mathbf{q} \rightarrow 0} K_{ij}(\mathbf{q}) = K_{ij}$.

However, in systems with long-range Coulomb interaction, the optical conductivity $\sigma(\mathbf{q}, \omega)$ at $\mathbf{q} \rightarrow 0$ limit depends on direction of \mathbf{q} due to the screening effect. For example, in three-dimensional isotropic systems, the longitudinal electric field $\mathbf{E}_{\text{ext}} \parallel \mathbf{q}$ induces the charge density modulation that screens the electric field, while the transverse electric field $\mathbf{E}_{\text{ext}} \perp \mathbf{q}$ does not induce such charge modulation. Therefore, the response to the longitudinal and transverse electric fields are different even in the limit of $\mathbf{q} \rightarrow 0$. Writing the optical conductivity as the sum of the longitudinal and transverse components as

$$\sigma_{ij}(\mathbf{q}, \omega) = \sigma_L(\mathbf{q}, \omega) \frac{q_i q_j}{q^2} + \sigma_T(\mathbf{q}, \omega) \left(\delta_{ij} - \frac{q_i q_j}{q^2} \right), \quad (38)$$

$\sigma_L(\mathbf{q} \rightarrow 0, \omega) \neq \sigma_T(\mathbf{q} \rightarrow 0, \omega)$ in general. Accordingly, the quantum weight in the limit of $\mathbf{q} \rightarrow 0$ depends on the direction of \mathbf{q} as well. By decomposing $K_{ij}(\mathbf{q})$ into the longitudinal and transverse components as

$$K_{ij}(\mathbf{q}) = K_L(\mathbf{q}) \frac{q_i q_j}{q^2} + K_T(\mathbf{q}) \left(\delta_{ij} - \frac{q_i q_j}{q^2} \right), \quad (39)$$

we have $K_L(\mathbf{q} \rightarrow 0) \neq K_T(\mathbf{q} \rightarrow 0)$ in general.

The static structure factor $S(\mathbf{q}) = (1/V)(\langle \rho(\mathbf{q})\rho(-\mathbf{q}) \rangle - \langle \rho(\mathbf{q}) \rangle \langle \rho(-\mathbf{q}) \rangle)$ is related to the longitudinal part of the optical conductivity [22]. Indeed, noting the continuity equation $\dot{\rho} + \nabla \cdot \mathbf{j} = 0$, and dissipation fluctuation theorem, one can show that the structure factor is related to K_L as

$$S(\mathbf{q}) = \frac{1}{2\pi} \mathbf{q}^T K_L(\mathbf{q}) \mathbf{q}. \quad (40)$$

Now let us consider the force acting on the probe's capacitor. Here we explicitly consider the position dependence of \mathbf{g}_I, \mathbf{g} with wavevector \mathbf{q} and carefully take the $\mathbf{q} \rightarrow 0$ limit. Since $\nabla g_C(\mathbf{r})$ is always longitudinal, i.e., $\mathbf{q} \parallel \nabla g_C$ in Fourier space, we have

$$\begin{aligned} F &= F_{n_p} + \frac{V}{2\epsilon S} \left(-\frac{\langle Q_0^2 \rangle}{V} + \frac{e^2}{2\pi} \mathbf{g} K'(\mathbf{q}) \mathbf{g} \right) \\ &= F_{n_p} + \frac{V}{2\epsilon S} \left(-\frac{\langle Q_0^2 \rangle}{V} + \frac{e^2}{2\pi} (\nabla g_C K'_L(\mathbf{q}) \nabla g_C + \mathbf{g}_I K'(\mathbf{q}) \mathbf{g}_I + \nabla g_C K'(\mathbf{q}) \mathbf{g}_I + \mathbf{g}_I K'(\mathbf{q}) \nabla g_C) \right) \end{aligned} \quad (41)$$

Further rewriting $\langle Q_0^2 \rangle$ with the structure factor by using Eq. (29) and combining it with Eq. (40) as well as assuming $\langle Q_0 \rangle \simeq 0$, we obtain

$$F = F_{n_p} + \frac{e^2 V}{4\pi\epsilon S} (\mathbf{g}_I K'(\mathbf{q}) \mathbf{g}_I + (\nabla g_C) K'(\mathbf{q}) \mathbf{g}_I + \mathbf{g}_I K'(\mathbf{q}) \nabla g_C) \quad (42)$$

Taking $\mathbf{q} \rightarrow 0$ limit yields the same expression as the results in the main text.

Nonadiabatic correction

Here we consider nonadiabatic corrections to the discussion in the main text. We start with the following Hamiltonian:

$$H_{\text{tot}} = H(\mathbf{A} = \mathbf{g}\hat{\varphi}) + H_p, \quad (43)$$

$$H_p = \frac{\hat{\varphi}^2}{2L_p} + \frac{\hat{q}^2}{2C_p}, \quad (44)$$

We assume \mathbf{g} is uniform and does not depend on position \mathbf{r} . We can include the effect of the scalar potential coupling by redefining \mathbf{g} and $H(\mathbf{A})$ as discussed in the previous section.

We denote the unitary transformation that diagonalizes $H(\mathbf{A})$ by U . U satisfies $U^\dagger(\mathbf{A})H(\mathbf{A})U(\mathbf{A}) = \sum_n E_n(\mathbf{A})|n\rangle\langle n|$ with $|n\rangle$ the eigenstate of $H(\mathbf{A})$. By applying $U(\mathbf{g}\hat{\varphi})$ to H_{tot} , we obtain

$$\tilde{H} \equiv U^\dagger H_{\text{tot}} U = \sum_n E_n(\mathbf{g}\hat{\varphi}) |n\rangle\langle n| + \frac{\hat{\varphi}^2}{2L_p} + \frac{(\hat{q} - \hbar\mathbf{g} \cdot \mathbf{a})^2}{2C_p} \quad (45)$$

where $\mathbf{a}_{mn}(\mathbf{A}) = i \langle m|\nabla_{\mathbf{A}}|n\rangle$ is the non-Abelian Berry connection. We write \tilde{H} as $\tilde{H} = H_{\text{ad}} + V$ where H_{ad} and V is given by

$$H_{\text{ad}} = \sum_n (E_n(\mathbf{g}\hat{\varphi}) + E_{\text{QG},n}) |n\rangle\langle n| + \frac{\hat{\varphi}^2}{2L_p} + \frac{(\hat{q} - Q)^2}{2C_p}, \quad (46)$$

$$V = -\frac{\hbar(\mathbf{g} \cdot \mathbf{a})}{C_p} \hat{q} + \mathcal{O}(g^2). \quad (47)$$

Here, $Q = \hbar\mathbf{g} \cdot \mathbf{a}_{\text{diag}}$ is proportional to the diagonal part of the Berry connection denoted by \mathbf{a}_{diag} , representing the induced charge in the circuit by the electronic system. H_{ad} is the adiabatic Hamiltonian and diagonal in the eigenbasis of $H(\mathbf{A})$, and it includes the quantum geometric potential for n -th eigenstate:

$$E_{\text{QG},n} = \frac{e^2}{2C_p} \mathbf{g} G_n \mathbf{g} \quad (48)$$

with (G_n) the many-body quantum metric for the n -th eigenstate. V is the off-diagonal in the eigenbasis of $H(\mathbf{A})$, representing the nonadiabatic correction that induces transitions between different eigenstates of $H(\mathbf{A})$. In V , we have neglected the commutator between \hat{q} and \mathbf{a} , which gives higher-order corrections in \mathbf{g} .

We treat $V \propto \mathbf{g}$ as a perturbation to H_{ad} . Up to the second order in \mathbf{g} , we can derive the effective Hamiltonian for the ground state with the Schrieffer-Wolff transformation as

$$H_{\text{eff}} = E_0(\mathbf{g}\hat{\varphi}) + E_{\text{QG},0} + \frac{\hat{\varphi}^2}{2L_p} + \frac{(\hat{q} - q_0)^2}{2C_p} + \Delta H_{\text{NA}} + \mathcal{O}(g^3), \quad (49)$$

$$\Delta H_{\text{NA}} = -\sum_{n \neq 0} \frac{\hbar^2}{C_p^2} \frac{(\mathbf{g} \cdot \mathbf{a}_{0n})(\mathbf{g} \cdot \mathbf{a}_{n0})}{E_n - E_0} \hat{q}^2 \quad (50)$$

where $q_0 = \hbar\mathbf{g} \cdot \mathbf{a}_{00}$ and E_n is the n -th eigenvalue of H . ΔH_{NA} is the nonadiabatic correction to the effective Hamiltonian, which arises from the virtual excitation to the excited states due to the nonadiabatic coupling V . Noting that the eigenstate under uniform \mathbf{A} is related to that at $\mathbf{A} = 0$ as $|n(\mathbf{A})\rangle = e^{-(ie/\hbar)\mathbf{A} \cdot \mathbf{R}} |n(0)\rangle$ with $\mathbf{R} = \sum_i \mathbf{r}_i$ the total position operator, we have $\mathbf{a}_{mn} = -(e/\hbar) \langle m|\mathbf{R}|n\rangle$. Using this, we can rewrite ΔH_{NA} as

$$\Delta H_{\text{NA}} = -\frac{e^2 \hat{q}^2}{C_p^2} g_i g_j \sum_{n \neq 0} \frac{\text{Re}[\langle 0|R_i|n\rangle \langle n|R_j|0\rangle]}{E_n - E_0} \quad (51)$$

We can show that ΔH_{NA} can be rewritten with the static polarizability χ_{ij} of the electronic system. The polarizability χ_{ij} is defined as

$$\mathbf{p} = \chi \mathbf{E}, \quad (52)$$

where \mathbf{E} is the applied electric field and \mathbf{p} is the induced polarization density. Note that χ is an intensive quantity. Using the Kubo formula, we can express χ_{ij} as

$$\chi_{ij} = \frac{2e^2}{\Omega} \sum_{n \neq 0} \frac{\text{Re}[\langle 0|R_i|n\rangle \langle n|R_j|0\rangle]}{E_n - E_0} \quad (53)$$

where Ω is the system volume. Comparing this with ΔH_{NA} , we find

$$\Delta H_{\text{NA}} = -\frac{\Omega}{2} \frac{\hat{q}^2 \mathbf{g} \chi \mathbf{g}}{C_p^2}. \quad (54)$$

ΔE_{NA} can be interpreted as the energy gain due to the dielectric response of the material to the fluctuating electric field generated by the circuit. The electric field generated by the circuit is given by $\hat{\mathbf{E}} = -\partial \hat{\mathbf{A}} / \partial t - \nabla \hat{\phi}$, which yields

$$\hat{\mathbf{E}} = -\mathbf{g}_I \dot{\hat{\phi}} - \nabla g_C \frac{\hat{q}}{C_p} = -\mathbf{g} \frac{\hat{q}}{C_p} \quad (55)$$

With this, we can rewrite the nonadiabatic correction as

$$\Delta H_{\text{NA}} = -\frac{\Omega}{2} \hat{\mathbf{E}} \chi \hat{\mathbf{E}} \quad (56)$$

This is nothing but the energy gain due to the dielectric response of the material to the fluctuating electric field generated by the circuit.

Plugging this into H_{eff} , we obtain

$$H_{\text{eff}} = E_0(\mathbf{g} \hat{\phi}) + E_{\text{QG},0} + \frac{\hat{\phi}^2}{2L_p} + \frac{(\hat{q} - q_0)^2}{2C_{p,\text{eff}}} + \mathcal{O}(g^3), \quad (57)$$

$$C_{p,\text{eff}} = C_p + \mathbf{g} \Omega \chi \mathbf{g}. \quad (58)$$

Here, the nonadiabatic correction renormalizes the capacitance of the circuit from C_p to $C_{p,\text{eff}}$. The renormalization of the capacitance can be understood as the increased inertia of the flux in the circuit due to the electronic system.

The eigenenergy of H_{eff} is given by

$$E_{n_p} = E_0(\mathbf{g} \hat{\phi}) + E_{\text{QG},0} + \hbar \omega_p (n_p + 1/2) = E_0 + E_{\text{QG},0} + \hbar \omega_p (n_p + 1/2) + \delta E_{\text{NA}} + \mathcal{O}(g^3), \quad (59)$$

$$\delta E_{\text{NA}} = -\hbar \omega_p (n_p + 1/2) \frac{\mathbf{g} \Omega \chi \mathbf{g}}{2C_p}, \quad (60)$$

where $\omega_{p,\text{eff}} = 1/\sqrt{L_p C_{p,\text{eff}}}$ and $\omega_p = 1/\sqrt{L_p C_p}$. δE_{NA} is the nonadiabatic correction to the eigenenergy. Importantly, the nonadiabatic correction δE_{NA} is always negative, and hence contribute to an attractive force between the circuit and the material.

δE_{NA} depends on the photon number n_p in the resonator, in contrast to the adiabatic quantum geometric energy that is independent of n_p . In addition, the nonadiabatic correction vanishes when $L_p \rightarrow \infty$ and $\omega_p \rightarrow 0$, i.e., in the DC limit. This is in sharp contrast to the adiabatic quantum geometric energy that remains finite even in the DC limit. δE_{NA} involves the static polarizability χ of the electronic system in analogous to the van der Waals force or the usual Casimir effect.

Since δE_{NA} is nonadiabatic correction, it scales differently with the energy gap of the material Δ . Noting that the static polarizability roughly scales with the ground state quantum metric G_0 as $\Omega \chi \sim e^2 G_0 / \Delta$, we find that the nonadiabatic correction $\delta E_{\text{NA}} \sim -\hbar \omega_p (e^2 / (2C_p))$

$$\delta E_{\text{NA}} \sim -(n_p + 1/2) \frac{\hbar \omega_p}{\Delta} \frac{e^2}{2C_p} \mathbf{g} G_0 \mathbf{g} \sim -(n_p + 1/2) \frac{\hbar \omega_p}{\Delta} E_{\text{QG},0} \quad (61)$$

Therefore, the nonadiabatic correction is much smaller compared to the quantum geometric energy $E_{\text{QG},0}$ when the energy gap Δ is much larger than the cavity frequency $\hbar \omega_p$.

Example: Superconducting resonator as a target

We can understand the geometric zero-point energy in a language more familiar in superconducting circuits as well. To this end, we replace the electronic system with another superconducting LC circuit. To distinguish the two circuits, we call the original circuit the “probe” and the other circuit replacing the electronic system the “target”. In this case, the coupling through the vector potential is equivalent to an inductive coupling in a circuit language. Indeed, the minimal coupling term $\mathbf{j} \cdot \hat{\mathbf{A}}$ becomes $\mathbf{j} \cdot \mathbf{g}\hat{\phi} = (\mathbf{j} \cdot \mathbf{g})L_p\hat{I}$ and therefore represents the current-current interaction, which is naturally interpreted as the inductive coupling with mutual inductance $M \sim gL_p$. Therefore, we can analyze the system as two inductively coupled superconducting LC circuits, described by the following Hamiltonian:

$$H_{\text{tot}} = \frac{1}{2} \begin{pmatrix} \hat{\Phi} & \hat{\varphi} \end{pmatrix} \begin{pmatrix} L & M \\ M & L_p \end{pmatrix}^{-1} \begin{pmatrix} \hat{\Phi} \\ \hat{\varphi} \end{pmatrix} + \frac{\hat{Q}^2}{2C} + \frac{\hat{q}^2}{2C_p}, \quad (62)$$

where $\hat{\Phi}, \hat{Q}$ are the flux and the charge of the target circuit satisfying $[\hat{\Phi}, \hat{Q}] = i\hbar$, L, C are the inductance and the capacitance of the target circuit, and M is the mutual inductance between the target and the probe.

Assuming that the frequency of the target is much larger than that of the probe, we can apply our theory to this system. We can rewrite the Hamiltonian as

$$H_{\text{tot}} = H_{\text{eff}}(g\hat{\varphi}) + \frac{\hat{\varphi}^2}{2L_p} + \frac{\hat{q}^2}{2C_p}, \quad (63)$$

where H_{eff} is the effective Hamiltonian for the target in the presence of inductive coupling $g = M/L_p$, given by:

$$H_{\text{eff}}(\phi) = \frac{(\hat{\Phi} - \phi)^2}{2L_{\text{eff}}} + \frac{\hat{Q}^2}{2C}. \quad (64)$$

Here $L_{\text{eff}} = L - gM$ is the effective inductance of the target. The eigenenergy of $H_{\text{eff}}(\phi)$ for a given ϕ is given by $E_n(\phi) = \hbar\omega_{\text{eff}}(n + 1/2)$ with $\omega_{\text{eff}} = (L_{\text{eff}}C)^{-1/2}$. H_{eff} in general includes the backaction from the probe to the target through the inductive coupling g . When the coupling is sufficiently weak so that $gM = M^2/L_p \ll L$, $L_{\text{eff}} \simeq L$ and thus the effect of the probe is only producing an electromagnetic field acting on the target.

With Eq. (64), we can perform exactly the same analysis as above and we find an additional zero-point energy as

$$E_{\text{QG}} = g^2 \frac{\langle \hat{Q}^2 \rangle}{2C_p} = \frac{g^2}{4} \frac{Z_p}{Z_{\text{eff}}} \hbar\omega_p \quad (65)$$

where $Z_{\text{eff}} = \sqrt{L_{\text{eff}}/C}$ and $Z_p = \sqrt{L_p/C_p}$. In this case, the polarization fluctuation of the target in Eq. (8) is given by $\langle \hat{Q}^2 \rangle$.

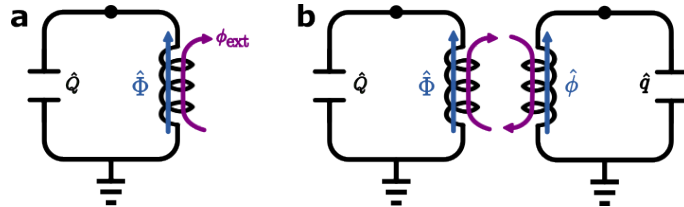


FIG. 3. Probing quantum metric with superconducting circuit. (a) A microwave resonator consisting of an inductor and a capacitor with an external magnetic flux ϕ_{ext} . (b) Two microwave resonators that are inductively coupled.